PHYSICAL REVIEW VOLUME 101, NUMBER 3 FEBRUARY 1, 1956

Optical Model Analysis of Scattering of 14-Mev Neutrons*

GLEN CULLER, SIDNEY FERNBACH, AND NOAH SHERMAN
Radiation Laboratory, Department of Physics, University of California, Livermore, California
(Received September 28, 1955)

Preliminary results for the scattering of 14-Mev neutrons using exact phase-shift calculations are presented. The model used consists of step-well potentials both with and without spin-orbit interactions.

INTRODUCTION

THE optical model of the nucleus[1] has been applied with considerable success to the scattering of nucleons by nuclei. The best correspondence between this model and experimental results was obtained for total neutron cross sections as a function of mass number of the scattering nucleus at moderately high energies.[1] A fairly complete analysis[2] of the experimental data for energies above 40 Mev was made using the WKB approximation which seemed successful at 90 Mev.

An exact phase-shift analysis in the low-energy region (1–3 Mev) was also successful in giving at least the qualitative features of the scattering cross sections both as a function of mass number and energy.[3]

At the intermediate energy of 14 Mev, there exist detailed experimental data on reaction cross sections and angular distributions of elastically scattered neutrons, as well as total cross sections. Corresponding calculations based on an optical model can be compared with these data and thus provide a sensitive test of the model. In this note, we report on the early results of such calculations, which were performed on the UNIVAC at this laboratory. In all cases, exact phase shifts were calculated.

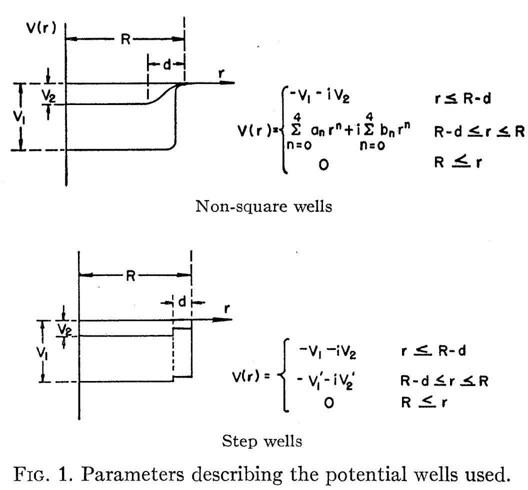

FIG. 1. Parameters describing the potential wells used.

DISCUSSION OF CALCULATIONS—STEP WELLS

The initial attempt to fit the 14-Mev scattering data by means of various choices of complex square-well potentials proved inadequate. The next attempt was made with the "nonsquare wells" shown in Fig. 1. The tail on this potential is a suitably chosen fourth degree polynomial in the radial variable. The tail on the real part of the potential need not be of the same functional form as that of the imaginary part, and indeed the best results were obtained with the imaginary tail falling off faster than the real tail. Calculations with such potentials were very time-consuming on the UNIVAC,

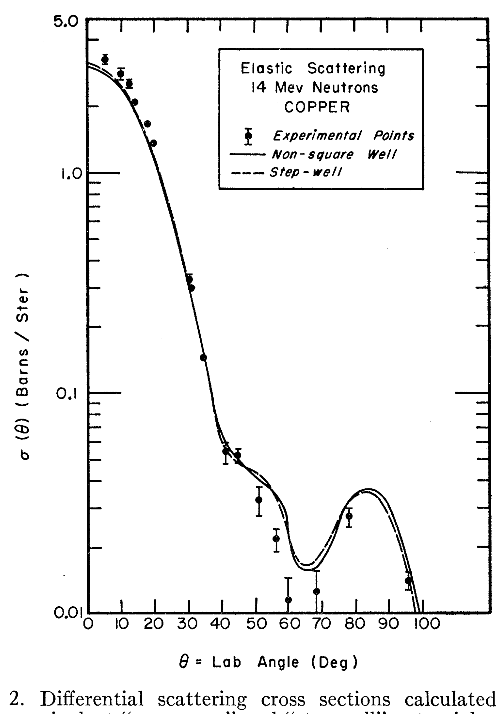

FIG. 2. Differential scattering cross sections calculated from equivalent "nonsquare" and "step-well" potentials.

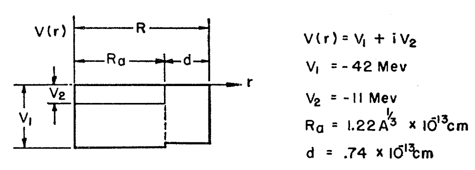

FIG. 3. Step-well potential which gives best agreement with experimental data.

* Work sponsored by the U. S. Atomic Energy Commission.
[1] Fernbach, Serber, and Taylor, Phys. Rev. **75**, 1352 (1949).
[2] T. B. Taylor, thesis, Cornell University, 1953 (unpublished).
[3] Feshbach, Porter, and Weisskopf, Phys. Rev. **96**, 448 (1954).

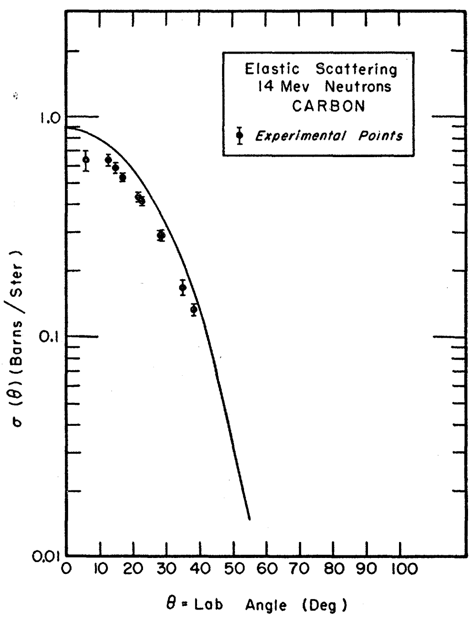

FIG. 4. Differential scattering cross section for carbon.

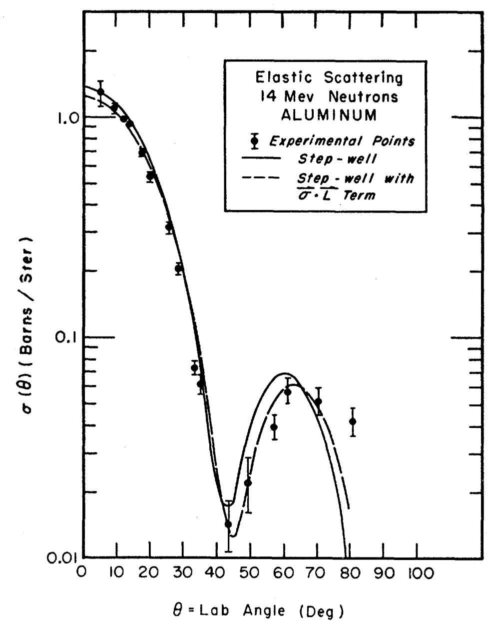

FIG. 6. Differential scattering cross section for aluminum.

so that equivalent "step walls" (Fig. 1) were used. The equivalent step well was taken to be identical with the nonsquare well in the region out to a radial distance, d, from the edge. Over the remaining distance the depth of the imaginary part was greatly reduced and the depth of the real part was kept the same or slightly reduced. The ratio between the edge distance, d, and the corresponding length of the nonsquare well's imaginary tail, was found to be $\sim$0.4. The equivalence of these potentials in fitting the data is shown in Fig. 2, where the differential cross sections derived from them appear to agree well within experimental accuracy. Other comparisons also demonstrated that the step-wells were equivalent to the polynomial-tail wells. Since the experimental results are not considered to be sufficiently accurate to warrant any preference between

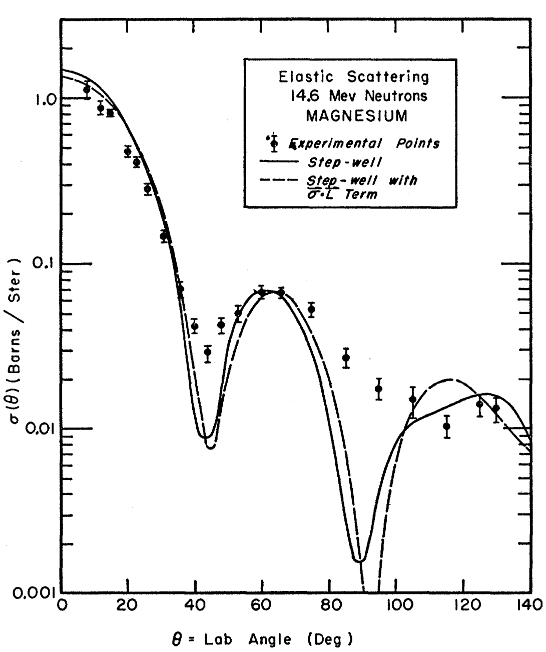

FIG. 5. Differential scattering cross section for magnesium.

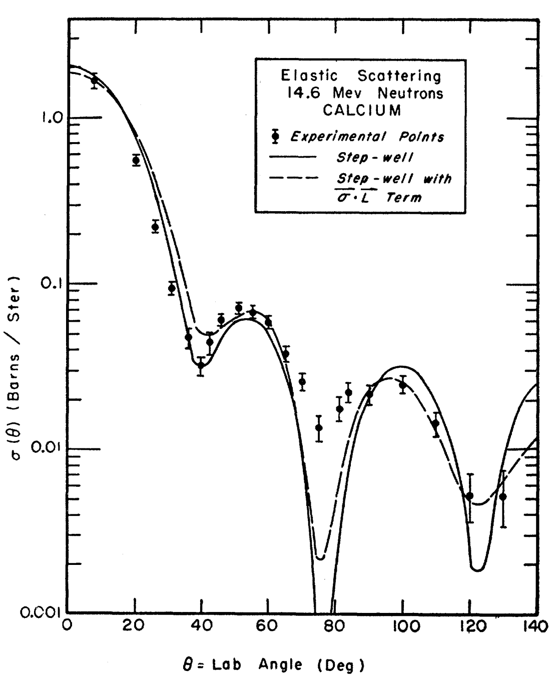

FIG. 7. Differential scattering cross section for calcium.

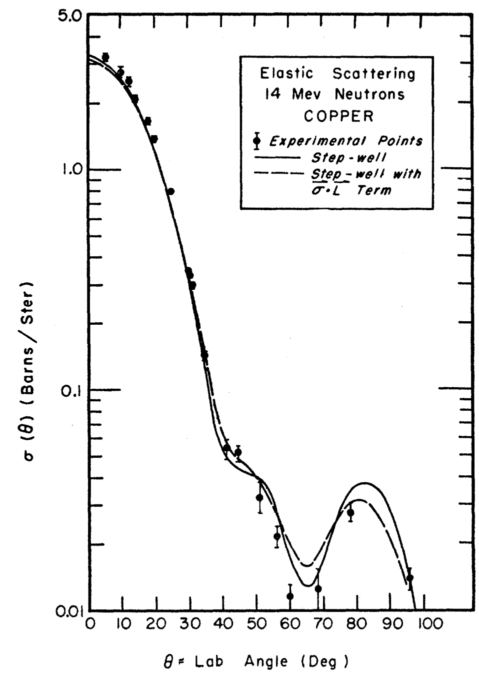

FIG. 8. Differential scattering cross section for copper.

these two well shapes, the subsequent calculations were performed with step wells.

The step well which yields the best over-all fit to the experimental data is shown in Fig. 3. The solid curves in Fig. 4 through Fig. 12 show angular distributions of elastically scattered neutrons for C, Mg, Al, Ca, Cu, Cd, Sn, Pb, and Bi, for which experimental data are available.[4,5] (These experimental results have not been corrected for multiple scattering, so that only qualitative agreement between theory and these data was

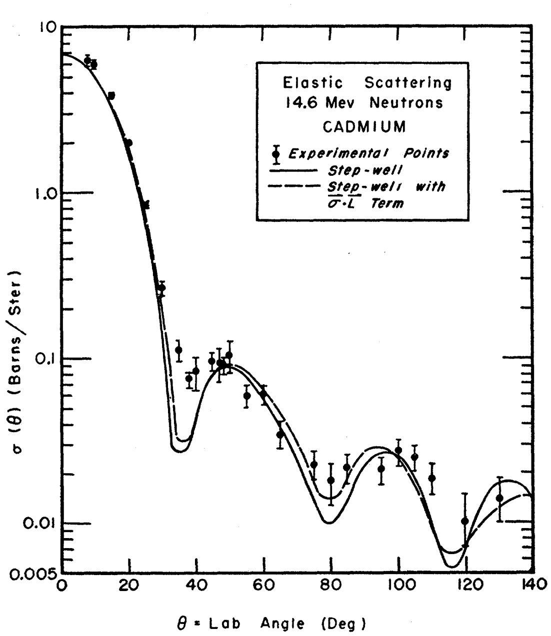

FIG. 9. Differential scattering cross section for cadmium.

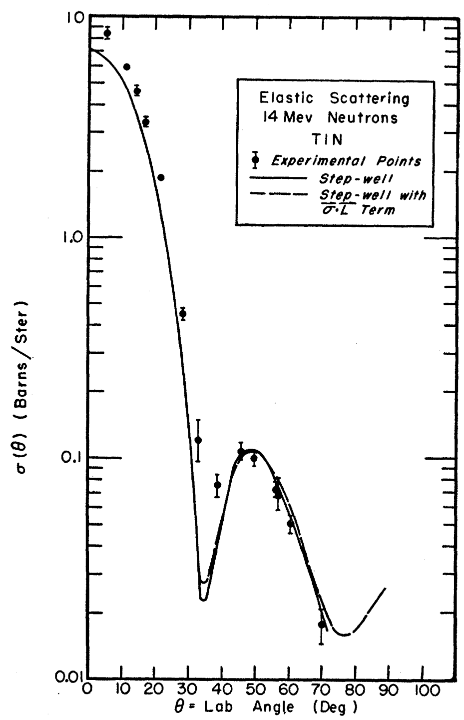

FIG. 10. Differential scattering cross section for tin.

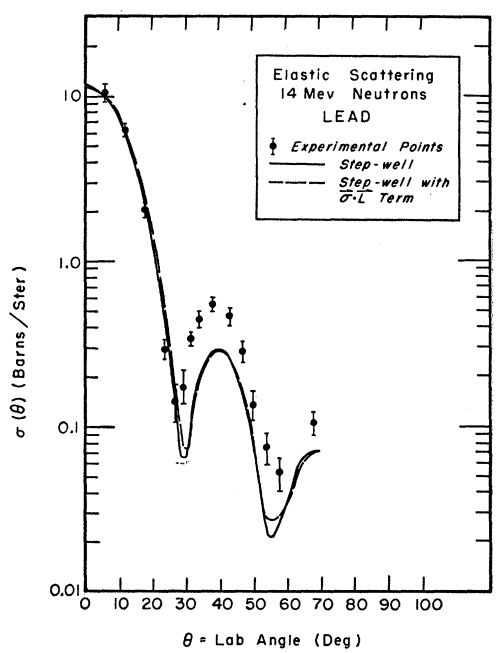

FIG. 11. Differential scattering cross section for lead.

[4] The elastic scattering angular distributions are tentative results communicated by J. Coon.

[5] William Cross, Chalk River (private communication).

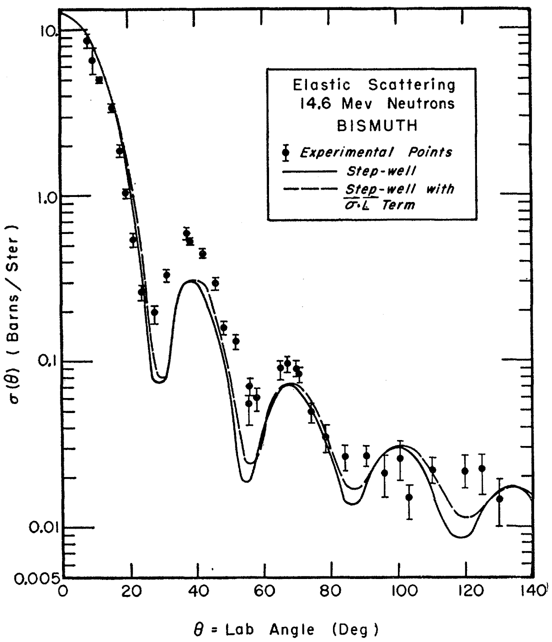

FIG. 12. Differential scattering cross section for bismuth.

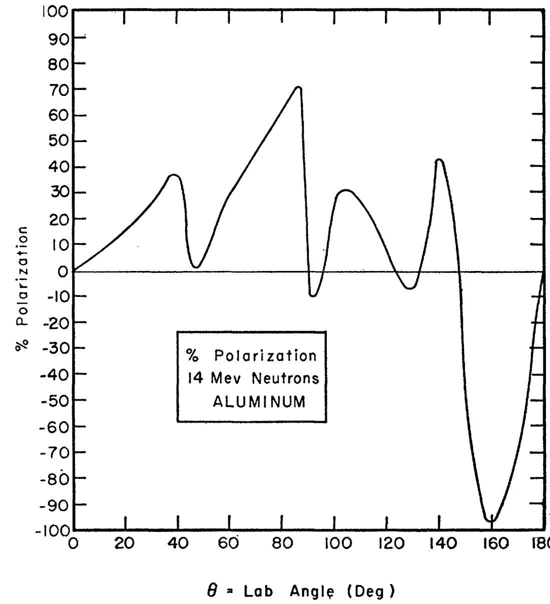

FIG. 14. Percentage polarization of primary beam after single scattering by aluminum.

attempted.) Figure 13 compares the theoretical and experimental results for reaction cross sections[6,7] and total cross sections.[7–9]

Although such pictures should not be taken too seriously, it is perhaps heuristic to interpret the shape of the best-fitting step-well in terms of nuclear structure. Since no "absorption" of the incident beam occurs in regions where the imaginary part of the potential is zero, we see that the edge, d, of the step well is such a region. The finite real potential produces elastic scattering, so that the edge can be regarded as a region in which the incoming neutron begins to experience nuclear forces and interacts with the nucleus as a whole. In the interior of the nucleus, within a radius R_a, the "absorption" describes inelastic scattering, corresponding to energy-transferring collisions with nucleons, and is accompanied by further elastic scattering. We can thus regard the radius R_a as describing the region containing nucleons which can be excited by the neutron and the larger radius R as representing the range of nuclear forces usually called the "nuclear radius."

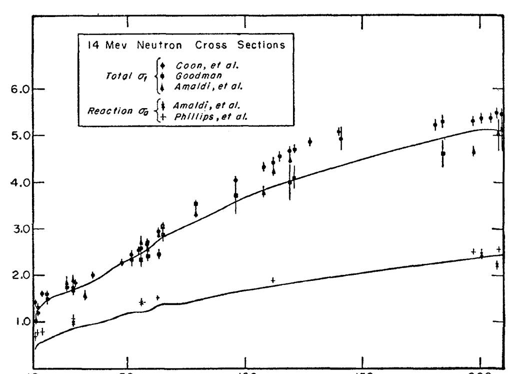

FIG. 13. Reaction and total cross section as function of mass number, A.

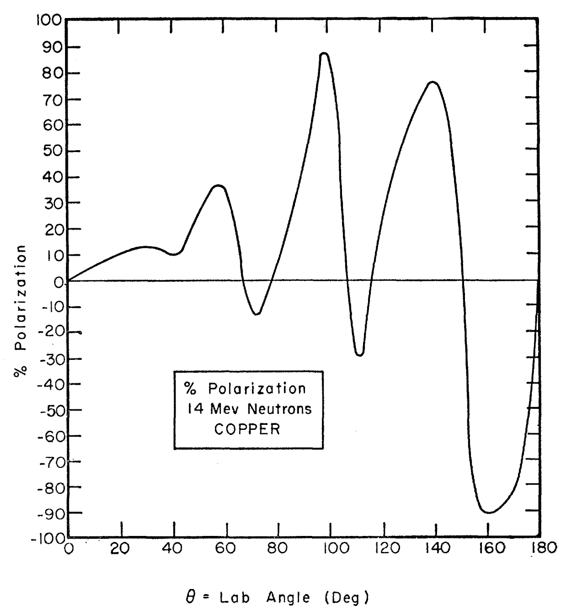

FIG. 15. Percentage polarization of primary beam after single scattering by copper.

[6] Phillips, Davis, and Graves, Phys. Rev. **88**, 600 (1952).
[7] E. Amaldi *et al.*, Nuovo cimento **3**, 203 (1946).
[8] Coon, Graves, and Barschall, Phys. Rev. **88**, 562 (1952).
[9] L. S. Goodman, Atomic Energy Commission Report AECU-1913, 1952 (unpublished).

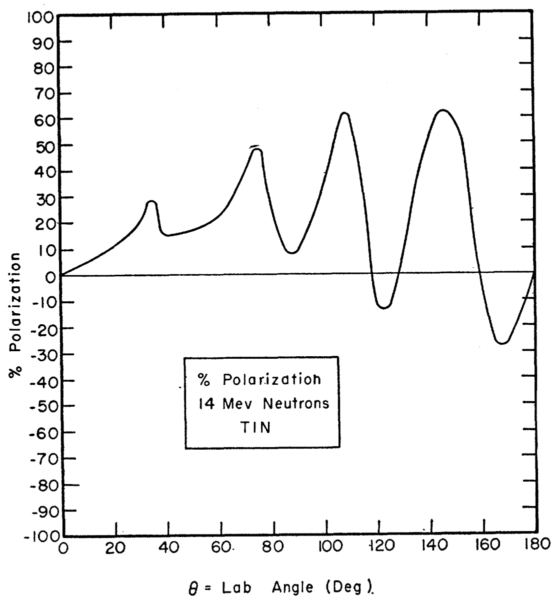

FIG. 16. Percentage polarization of primary beam after single scattering by tin.

Since $R_a=1.22\times10^{-13}A^{\frac{1}{3}}$ cm and $R=(1.22A^{\frac{1}{3}}+0.74)\times10^{-13}$ cm$\cong1.45\times10^{-13}A^{\frac{1}{3}}$ cm, for medium range A, both of these parameters fall within the range of nuclear radii as derived from a variety of experiments.

DISCUSSION OF CALCULATIONS—STEP WELLS WITH SPIN-ORBIT INTERACTION

The effect of adding a spin-orbit interaction term to the real part of the potential was investigated to see what effect it would have on the scattering cross

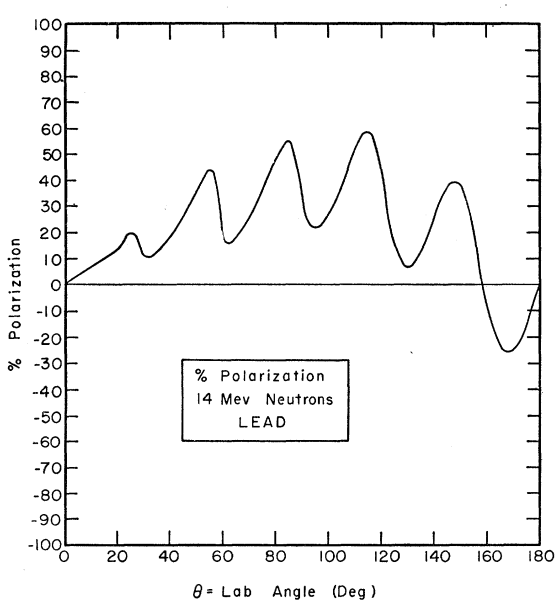

FIG. 17. Percentage polarization of primary beam after single scattering by lead.

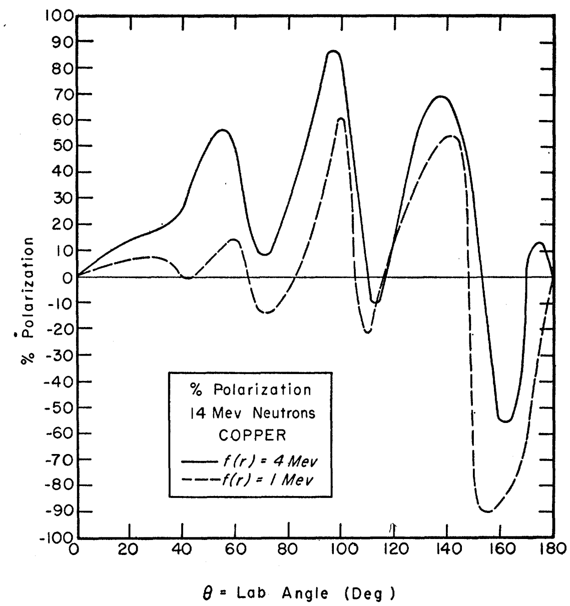

FIG. 18. Comparison of polarization curves for copper using $f(r)=1$ and 4 Mev.

sections. This additional term was tried in the form of $f(r)\boldsymbol{\sigma}\cdot\mathbf{L}$, where $f(r)$ was considered constant and of the order of 2 Mev in the region R_a to R. Putting the $\boldsymbol{\sigma}\cdot\mathbf{L}$ with a coefficient of 2 Mev on this edge seemed to be equivalent to taking its coefficient equal to $\frac{1}{4}$ Mev when taken over the entire nucleus so far as any significant differences in the angular distributions were concerned. In the figures contained in this report, the spin-orbit term appears only over the edge, a region of 0.74×10^{-13} cm.

The results of these calculations are shown as broken-line curves in Fig. 5 through Fig. 12. Figures 14 through Fig. 17 show the percent polarization of the primary

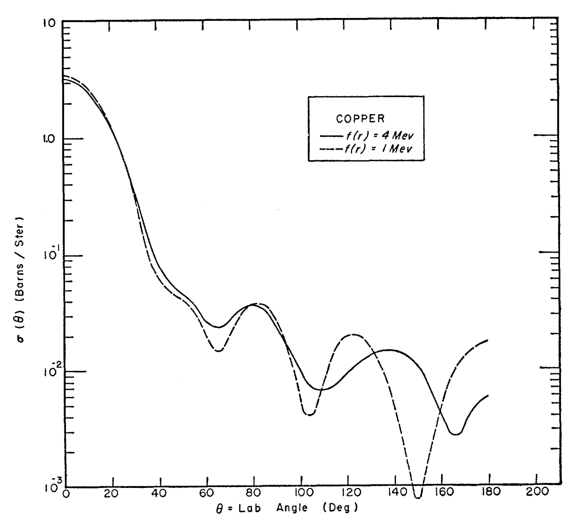

FIG. 19. Comparison of elastic scattering curves for copper using $f(r)=1$ and 4 Mev.

beam after a single scattering. It is apparent that the effect on the angular distribution is slight when $f(r)\approx 2$ Mev. The polarization curves show fairly low percentage polarization for small angles, but the structure indicates a greater average positive polarization for larger mass numbers. It is interesting that this polarization is positive for small angles rather than negative as it is at higher energies ($\sim$300 Mev).[10] Figure 18 shows the effect of varying $f(r)$ from 1 to 4 Mev and Fig. 19 shows the corresponding effect on the angular distribution. The most significant effect on the angular distribution seems to be the damping of the diffraction oscillations with increasing $f(r)$.

Further scattering calculations are being made for different energies, for incident neutrons and protons, both with and without the spin-orbit term. A new UNIVAC calculation providing for potential of arbitrary shape is now in use. The results of these calculations will be made available as soon as feasible.

[10] Fernbach, Heckrotte, and Lepore, Phys. Rev. **97**, 1059 (1955).

PHYSICAL REVIEW VOLUME 101, NUMBER 3 FEBRUARY 1, 1956

Low-Lying Levels of P^{30}

C. Broude, L. L. Green, J. J. Singh, and J. C. Willmott
Nuclear Physics Research Laboratory, University of Liverpool, Liverpool, England

(Received September 26, 1955)

New states in P^{30} are identified by determination of γ-ray energies from the reaction $Si^{29}(p,\gamma)P^{30}$. The angular distributions of transitions to the ground and first excited states have been determined and spins and parities assigned on the basis of these measurements. The first excited state is thus identified as the first $T=1$ state of P^{30}.

The lowest lying states of isotopic spin $T=0$ and $T=1$ in $A=4n+2$ nuclei have been surveyed by Moskowski and Peaslee.[1] The first $T=1$ state of the nucleus P^{30}, which is one of this series, has not previously been identified with certainty. Using a reasonable value of the nuclear radius, Moskowski and Peaslee predict that this state should be at approximately 500 kev above the ground state.

Endt, Kluyver, and Van der Leun[2] have observed γ-ray transitions involving a state at 0.688 ± 0.007 Mev in the reaction $Si^{29}(p,\gamma)P^{30}$. They studied this reaction at resonances occurring at proton energies of 414 kev and 326 kev, but were unable to determine the spin and parity of the 0.688-Mev state with certainty and so establish the isotopic spin of this state.

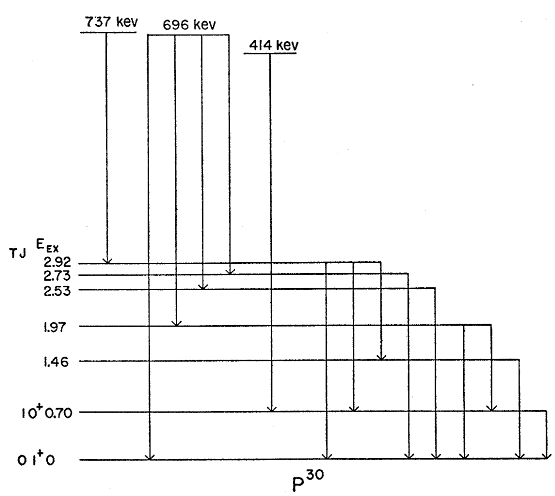

Fig. 1.

Using NaI scintillation spectrometer techniques, which have been described in a previous paper,[3] we have studied the γ radiation from the $Si^{29}(p,\gamma)P^{30}$ reaction at three resonances occurring at proton energies 737 kev, 696 kev, and 414 kev. The γ-ray energies observed fitted into the decay scheme shown in Fig. 1. This decay scheme was checked at each resonance by intensity and coincidence measurements. New states in P^{30} are observed at 1.46, 1.97, 2.53, 2.73, and 2.92 Mev.

At the 414-kev resonance, the angular distribution of 5.33-Mev γ ray and the 690 ± 10 kev γ ray involved in the cascade, resonance level$\rightarrow$690-kev state$\rightarrow$ground state, have been observed. The 690-kev γ ray is isotropic. This could be due to (a) the resonance being formed by s-wave protons or (b) the formation of a $J=0^+$ resonant state by s- or p-wave protons or (c) the 690-kev state itself being $J=0^+$. The first two possibilities are ruled out by the observation that the 5.33-Mev γ ray which feeds the 690-kev state from the resonance level is not isotropic but has a strong angular distribution of the form $1-0.3\cos^2\theta$. These results can only be explained if the 690-kev state has spin and parity 0^+ and can therefore be identified with certainty as the first $T=1$ state of P^{30}.

The separated Si^{29} target was provided by the Atomic Energy Research Establishment, Harwell. We wish to thank Professor H. W. B. Skinner for his encouragement and advice.

[1] S. A. Moskowski and D. C. Peaslee, Phys. Rev. **93**, 455 (1954).
[2] Endt, Kluyver, and Van der Leun, Phys. Rev. **95**, 580 (1954).
[3] Green, Singh, and Willmott, Phil. Mag. (to be published).